AN IMPROVED SUPERCONDUCTING ADS DRIVER LINAC DESIGN

R.W. Garnett, F.L. Krawczyk, G.H. Neuschaefer
Los Alamos National Laboratory, Los Alamos, New Mexico

Abstract

In this paper we discuss recent work to further improve our superconducting (SC) ADS driver linac design. Our design assumes use of the 6.7-MeV LEDA RFQ as an injector to the SC driver linac. We have examined the feasibility of accelerating a 20-mA CW beam to 600 MeV using only 350-MHz SC multi-spoke resonator cavities operating at 4 K. Replacing the 2 K, 700-MHz SC elliptical cavity sections with spoke resonators has several advantages, including reduced cryo-plant operating cost and an improved real-estate accelerating gradient due to the longer active lengths of the 350-MHz cavities. We discuss the details of the new design layout and beam dynamics simulations, including effects due to operational and alignment errors. Preliminary cavity modelling results for the proposed five-gap spoke resonators are also discussed. This accelerator design would be appropriate as a driver linac for applications such as waste transmutation, fusion materials testing, etc.

Introduction

In this paper we discuss the results of a feasibility study to design an ADS driver linac to accelerate a 20-mA CW beam to 600 MeV using only 350-MHz superconducting (SC) spoke resonator cavities operating at 4 K. This design work is primarily an extension of the final all-SC design completed for the Accelerator Production of Tritium (APT) Project [1] which was initially based on other previous work for APT/AAA [2,3]. Replacing the 2 K, 700-MHz SC elliptical cavity sections with spoke resonators has several advantages including reduced cryo-plant operating cost and an improved real-estate accelerating gradient due to the longer active lengths of the 350-MHz cavities. We discuss the details of the new design layout and beam dynamics simulations, including beam matching, and effects due to operational and alignment errors. Preliminary cavity modelling results for the five-gap resonators to be used in the high-energy section of the linac are also discussed.

Design details

Our superconducting (SC) linac design is based on the APT design discussed in Ref. [1] with the replacement of the $\beta = 0.48$ and $\beta = 0.64$ elliptical SC cavities with five-gap (four-spoke) spoke resonator cavities. The $\beta = 0.82$ section of the linac has been eliminated due to the reduced final beam energy of 600 MeV. In this example design we have used SC solenoids inside each cryomodule for transverse focusing instead of transitioning to room-temperature doublets at high energy as was done for APT. Table 1 gives the linac parameters for this design. Figure 1 shows schematic layouts of the cryomodules for each section along with the present RF configuration. A detailed layout of the cryomodule was completed in an earlier study [4]. The cryomodule parameters determined from that study are assumed here also.

Specific phase and accelerating gradient ramps are used to adiabatically capture the Low-energy Demonstration Accelerator (LEDA) RFQ beam [5] and to make the transitions from section-to-section as current insensitive as possible. These ramps have been modified from our previous design in order to match between the newly introduced spoke cavity sections. As can be seen in Figure 1, in Section 1 it has been assumed that each cavity is driven by a separate RF generator. In the other sections, two or three cavities will be driven per RF generator. For these sections it is assumed that the phases can be set individually for each cavity, however, each set of cavities driven by a single RF generator must receive the same power (split equally).

Just as in our previous design, it is assumed that Sections 1 and 2 will be powered by commercially available inductive output tubes (IOTs). However, the power required per cavity in Sections 3 and 4, assuming 20-mA operation and the selected accelerating gradients, exceeds the operating limits of all presently available IOTs. As a result, klystrons will be used to provide RF power to these cavities. The maximum power required for a cryomodule is 408 kW for Section 3 and 560 kW for Section 4. Figure 1 presently shows a three-way split between cavities in these cryomodules. This is naturally based on the total number of cavities in each section being divisible by three. However, a four-way split could save substantial RF system costs (25-33%) and still allow a conservative operating margin for the klystrons [6].

Figure 2 shows the synchronous phase ramping used in our design. Figures 3 and 4 show the transit-time factor and E_0T, respectively, as a function of beam energy along the linac. Figures 5 and 6 show the transverse and longitudinal zero-current phase advances per period and per unit length for this design.

Table 1. SC linac design parameters

	Section 1	Section 2	Section 3	Section 4	Total
Structure type	Two-gap spoke	Three-gap spoke	Five-gap spoke	Five-gap spoke	
Frequency (MHz)	350	350	350	350	
Cavity geometric beta	0.175	0.34	0.48	0.64	
Cavity bore radius (cm)	2.5	3.0	3.0	3.0	
L-cavity (active) (m)	0.100	0.333	0.826	1.100	
L-cavity (physical) (m)	0.200	0.433	1.101	1.371	
L-magnet-to-cavity (m)	0.300	0.300	0.300	0.300	
L-magnet (m)	0.150	0.150	0.250	0.400	
L-warm-to-cold-1 (m)	0.394	0.394	0.394	0.394	
L-warm-to-cold-2 (m)	0.419	0.419	0.419	0.419	
L-warm-space (m)	0.300	0.300	1.413	1.413	
L-cryomodule (m)	4.226	6.624	5.266	6.226	
L-cryoperiod (m)	4.526	6.924	6.679	7.639	
L-focusing period (m)	2.263	3.462	6.679	7.639	
Cav/cryomodule	4	6	3	3	
Cav/section	80	36	21	39	176
No. of cryomodules	20	6	7	13	46
DW/cav (MeV)	0.08-0.64	0.48-2.11	4.20-6.81	8.81-9.33	
Synchronous phase ( )	-45 to -32	-32 to -28.4	-28	-28	
E_0T (MV/m)	1.13-7.51	1.71-7.50	4.63-7.50	7.28-7.71	
Win, section (MeV)	6.70	43.12	112.01	239.30	
Wout, section (MeV)	43.12	112.01	239.30	600.03	
DW/section (MeV)	36.42	68.89	127.29	360.73	
Section length (m)	90.52	41.54	46.75	96.31	278.12
Max. coupler power @ 20 mA (kW)	12.7	42.9	136.0	187.0	
No. of cavities/RF generator	1	2	3	3	
No. RF generators/ section	80	18	21	39	158
Magnet type	SC solenoid	SC solenoid	SC solenoid	SC solenoid	
Magnet field	1.55-3.32 T	3.84-4.36 T	3.96-4.84 T	4.16-5.88 T	
Average RE gradient (MV/m)	0.40	1.66	2.72	3.63	2.13

Figure 1. Schematic cryomodule layouts for each superconducting linac section

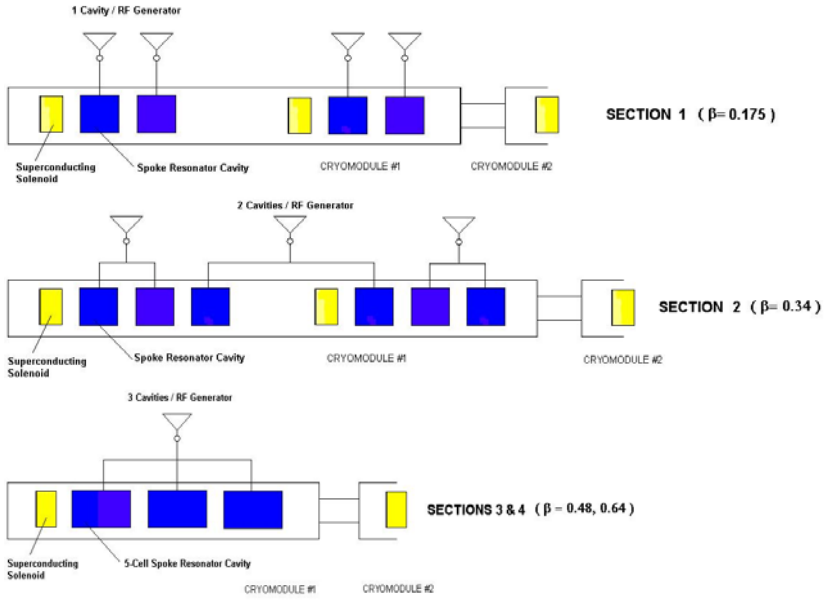

Figure 2. Synchronous phase as a function of beam energy along the linac

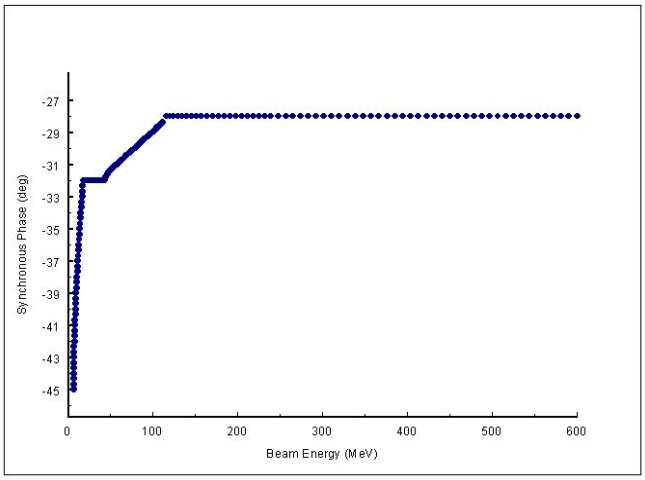

Figure 3. Transit time factor as a function of beam energy along the linac

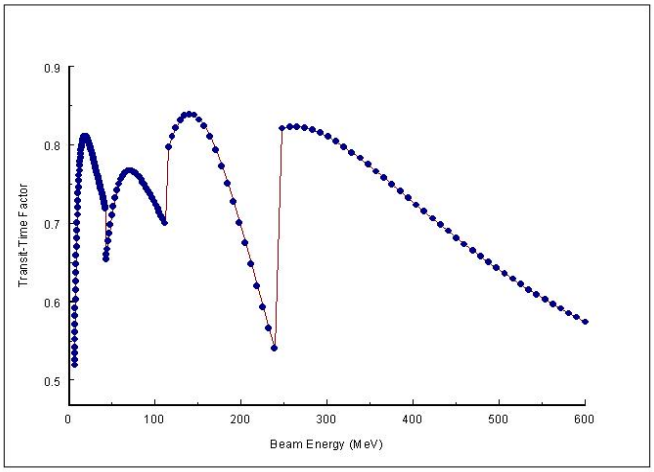

Figure 4. E_0T as a function of beam energy along the linac

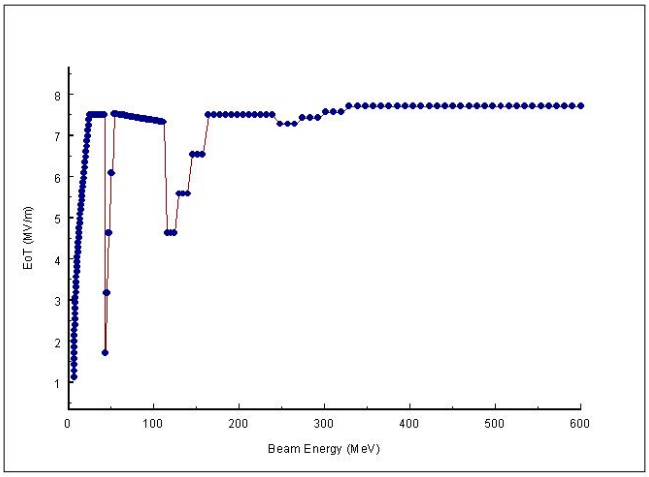

Figure 5. Zero-current phase advances per period as a function of beam energy along the linac

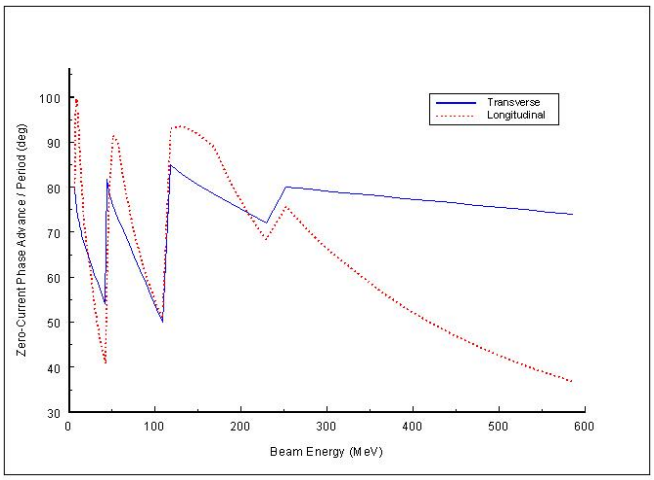

Figure 6. Zero-current phase advances per unit length as a function of beam energy along the linac

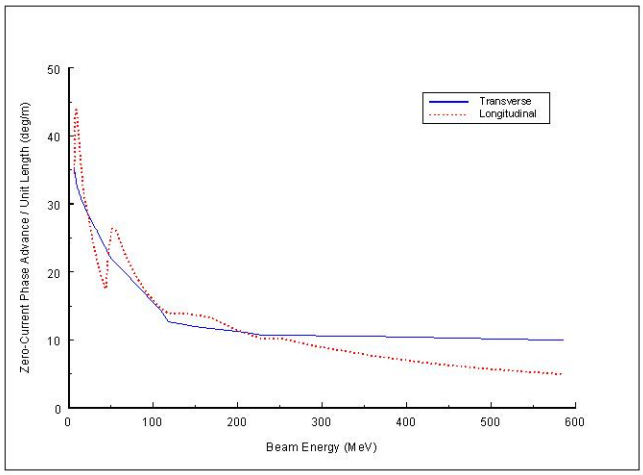

Examination of Table 1 shows that the use of five-gap spoke resonator cavities in the higher-energy sections of the linac significantly increases the real-estate accelerating gradient. An improvement of a factor of approximately 2.4 in the 112-600 MeV sections of the linac is observed as compared to previous designs using 700-MHz elliptical cavities. This is primarily due to the increased active cavity length at the lower operating frequency.

The expected performance of the $\beta = 0.175$, two-gap cavities has already been well-documented based on both calculations and measurements of a prototype cavity [7,8]. Performance of the $\beta = 0.34$, three-gap cavities has been estimated based on these results [9]. The details of the five-gap cavity design are discussed later in this paper. The maximum accelerating gradient used in this design is 7.7 MV/m, which seems reasonable based on the measurement results for the two-gap cavities.

An integrated mechanical and RF design for a power coupler was completed for the $\beta = 0.175$, two-gap spoke resonator cavities [10]. The power will be coupled electrically into the cavities using a coaxial-type coupler design. The direct coupling of the RF power into the cavity reduces the RF losses

and thereby maintains the overall RF efficiency of the spoke resonator cavities. The use of a single power coupler per cavity is the preferred approach based on preliminary estimates that indicate that the introduction of a second coupler significantly degrades the performance of the cavity. The maximum CW power per coupler is expected to be approximately 190 kW in Sections 3 and 4, where the five-gap cavities are used. At this power level, additional power coupler development may be necessary to meet the requirements for this design.

For our study we examined two schemes to match the LEDA RFQ beam into the SC linac at 6.7 MeV. The first scheme uses a more conventional approach and does not require any modification of the LEDA RFQ. It uses six magnetic quadrupoles and two RF bunching cavities to transform the RFQ output beam. Therefore, eight parameters must be varied and properly set to achieve the matching conditions. However, this scheme was found to be not very effective.

The second scheme requires modification of the last section of the LEDA RFQ to produce a round beam at the exit. This is desirable since the matched beam into a solenoid focusing system is round. The exit section of the RFQ must be increased from 6 cm in length to approximately 30 cm to achieve this. To maintain the present overall RFQ tank length and therefore minimise the required RFQ modifications, the increase in exit section length is achieved by removing a few accelerating cells in the last section of the RFQ. New RFQ vanes would need to be manufactured for the last section.

Removal of a few accelerating cells will reduce the RFQ output energy from 6.7 MeV to 6.5 MeV. If necessary, this 0.2 MeV energy difference can easily be compensated for in the high-energy end of the SC linac to recover the final desired 600-MeV linac output energy. This scheme uses two RF bunching cavities, a matching solenoid, and the first solenoid of the SC linac to achieve the matching conditions. This solution requires control or variation of only four parameters to perform matching.

The cryomodule layouts shown in Figure 1 were determined primarily by mechanical engineering constraints. Because of the relatively long focusing periods that result as a consequence, it will probably not be possible to design a completely current-insensitive matching section between the RFQ and the SC linac. The LEDA RFQ has both strong transverse and longitudinal focusing. The transverse focusing strength (zero-current transverse phase advance) per unit length in this RFQ is approximately 1.96 /cm. The focusing strength per unit length at the front-end of the SC linac is approximately 0.336 /cm, a factor of 5.8 weaker. Either weaker focusing in the RFQ or stronger focusing in the SC linac would be required to allow a nearly current insensitive matching section to be designed. Weakening the RFQ focusing will tend to destroy the beam quality and may not be desirable. We studied the effect of reducing the longitudinal focusing at the RFQ exit and found no improvement in the ease of matching or beam capture at high beam currents. It appears that stronger longitudinal focusing per unit length in the SC linac is required to allow operation at high beam currents as discussed in our previous report [1].

Simulation results

All beam dynamics simulations were carried out using 10 000 macroparticles. The PARMTEQM code was used to perform the RFQ simulations. A matched input beam distribution was generated in the code. The beam was then propagated through the RFQ and the desired matching section configuration. The PARMTEQM output beam distribution was then read into the LINAC code. This code was used to simulate the SC linac. Simulations for the ideal linac, with no errors, were performed along with cases including the full range of alignment and RF errors as previously specified for the APT project. LEDA injector data was used to determine the RFQ input emittances to be used in the simulations [11]. Table 2 shows the LEDA beam emittances for various currents.

Table 2. RFQ input and output emittances

Current (mA)	In (p-cm-mrad)	Out-ϵ_x (p-cm-mrad)	Out-ϵ_y (p-cm-mrad)	Out-ϵ_L (deg-MeV)
0	0.0060	0.01324	0.01390	0.2866
20	0.0072	0.01778	0.01778	0.1860
100	0.0122	0.03036	0.03050	0.2115

Simulations were carried out for the ideal linac for 0 mA, 20 mA, and 100 mA to check the current insensitivity of the matching scheme and the performance of the linac, including beam losses. The matching section parameters were set to the 20-mA matched beam settings. Beam losses were observed for the 100-mA case, however, the linac performance is acceptable for 20 mA.

Simulations with alignment and RF errors were performed for 20 mA only. A set of twenty 10 000-macroparticle simulations, each having a different set of random errors, was run. The magnitudes of the errors were assumed to be identical to those used for the baseline APT design and are shown in Table 3. Solenoid fringe fields extending out to a distance equal to the solenoid aperture radius were also included. Figure 7 shows the maximum beam amplitude as a function of beam energy including the full set of alignment and RF errors. All 20 simulation runs are plotted so that the spread in values can be observed. Only 15% of the runs exhibited beam loss. Of those runs, all had losses of 10^{-4}, all occurring in Section 1 of the linac. The RF errors were found to cause the observed beam loss. Reducing the magnitudes of the RF errors somewhat did not eliminate the losses. Section 1 of the linac will need improvement to further minimise or eliminate the beam loss and to allow a sufficient operating margin with achievable operational errors. Additionally, the transverse emittance of the beam was found to be well-behaved in spite of the small longitudinal beam losses; due to random errors, it grew approximately 30% during the simulations. The effects of component failures in the linac were not studied. Such a study, including compensation methods, could be carried out after additional design optimisation has been completed.

Table 3. Random errors used in the superconducting linac simulations

Description of error	Random error value (–)
Solenoid transverse displacement (x and y)	0.25 mm
Solenoid tilt	0.16 mrad
Solenoid field strength	0.25%
Cavity transverse displacement (x and y)	0.75 mm
Klystron amplitude (static error)	2.0%
Klystron phase error (static error)	2.0
Cavity amplitude error (static error)	5.0%
Cavity phase error (static error)	5.0
Klystron amplitude (dynamic error)	1.0%
Klystron phase (dynamic error)	1.0
Cavity amplitude (dynamic error)	5.0%
Cavity phase (dynamic error)	5.0

Figure 7. Maximum beam amplitude as a function of beam energy along the linac for 20 mA and all errors

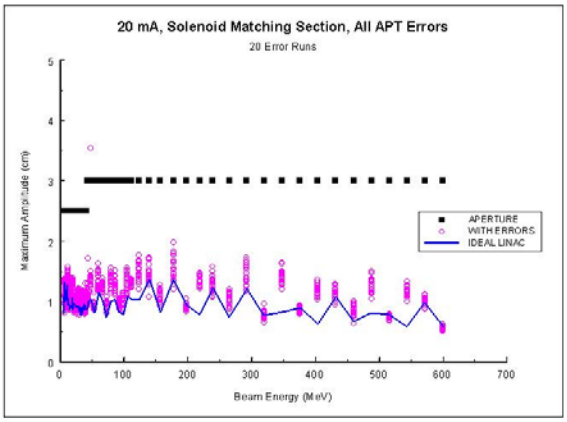

Preliminary five-gap multi-spoke resonator design

The possibility of replacing five-cell elliptical resonators at $\beta = 0.48$ and $\beta = 0.64$ with spoke resonators having the same number of cells has been investigated. A preliminary design and optimisation of candidate spoke geometries was done with Microwave Studio (MWS). The results of this study were used to provide transit time factor data for the design and the beam dynamics simulations presented earlier. The active lengths of the five-gap spoke resonators were found to be approximately 60% longer than the equivalent elliptical cavities at 700 MHz.

Some cavity optimisation was attempted. The spoke cross-section was optimised using a mid-cell and appropriate boundary conditions for the π-mode. The optimised spokes were then used to assemble a full five-gap (four-spoke) resonator. Figure 8 shows the full $\beta = 0.48$ geometry. Note that the end-cells are approximately half the length of the inner cells. This is required to produce flat fields along the structure, as also shown in Figure 8. These same techniques have been fully demonstrated for the $\beta = 0.175$ spoke resonator we built and tested in 2002 [12]. A parameter study was also done to simultaneously minimise peak electric and peak magnetic fields. Each geometric change also changed the frequency of the structure. To compare structures with the correct frequency, MWS was allowed to automatically re-tune the frequency close to 350 MHz by correcting the cavity radius. The parameters varied in the study were the radius of the spoke base, the width of the racetrack and the thickness of the racetrack. Table 4 gives the RF-parameters of the five-gap cavities after some optimisation.

Figure 8. Full five-cell model of the $\beta = 0.48$ spoke resonator. The on-axis electric field is also shown.

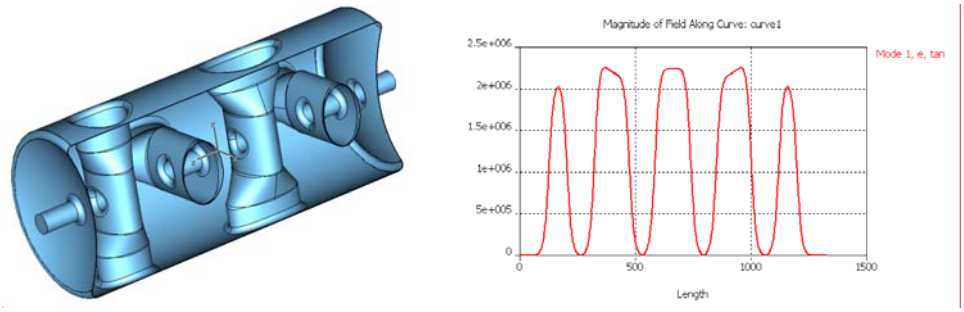

Table 4. RF-parameters for the β = 0.48 and 0.64, five-gap spoke resonators

	β = 0.48	**β = 0.64**
Frequency	350 MHz	350 MHz
R_s	4.893 mΩ	4.846 mΩ
Q_0 (RT)	18 200	19 430
Q_0 (4 K, 60 nΩ)	1.484E+09	1.584E+09
G	89.07 Ω	94 Ω
P_{cav} (4 K, 60 nΩ)	1.51 W	1.40 W
U	0.5 J	0.5 J
Active length	0.833 m	1.0871 m
Length (flange-to-flange)	1.109 m	1.303 m
Voltage	1.501 MV	1.52874 MV
E_0T	1.8019 MV/m	1.4063 MV/m
Transit-time factor	0.818	0.817
E_p/E_0T	3.49	3.74
B_p/E_0T	11.62 mT/MV/m	11.56 mT/MV/m
B_p/E_p	3.33	3.09
E_p/E_{0Ave}	2.86	3.06

In order to further improve on our preliminary cavity design, we will need to examine and take advantage of approaches used by other groups [13] that might ameliorate the performance of the multi-gap spoke resonators. We have already taken advantage of the dish-shaped end walls such as those used in the ANL designs [14]. We have also used different spoke shapes at the ends and middle of the resonator to tailor the spoke shapes to better accommodate the magnetic field pattern along the structure. Other methods of improvement, such as using a rectangular cavity body as proposed by FZ Jülich [15] (making more room for the magnetic field around the spoke base), should also be examined.

Summary

A design for an all-SC linac using only spoke resonator cavities to accelerate a 20-mA beam to 600 MeV for ADS applications has been completed. Our study has shown that replacing the 700-MHz elliptical cavities with 350-MHz, five-gap spoke resonator cavities offers many significant improvements to our previous design, the most important of which is the improved real-estate accelerating gradient resulting from a shorter overall linac length. Operational cost savings should also be realised by the elimination of the 2 K elliptical cavities and their associated cryo-plant. A particular beam dynamics and operational advantage is the larger longitudinal acceptance that is maintained throughout the linac by operating only at 350 MHz and thereby reducing the effects of RF errors.

Some additional design optimisation is desired, however. We continue to observe beam losses in the lowest-energy section of the SC linac when random alignment and operational errors are included. To further improve this section of the linac, we will examine an alternative RFQ design optimised for 20-mA operation and consider the possibility of using other, more compact SC structures in the first section. Additionally, the choice of geometric-β for the five-gap cavities should be re-evaluated to see if further improvements in the transit time factors are possible. Testing of a prototype five-gap cavity would also be desirable.

REFERENCES

[1] Garnett, R. and G. Neuschaefer, *APT SC Linac Design and Beam Dynamics*, Los Alamos National Laboratory Memorandum, LANSCE-1:01-075, 13 September 2001.

[2] Garnett, R., *ADTF Superconducting Design*, Los Alamos National Laboratory Memorandum, LANSCE-1:01-047, 1 May 2001.

[3] Garnett, R., *ADTF Superconducting Linac Design – Viability of Reducing Number of Spoke Sections*, Los Alamos National Laboratory Memorandum, LANSCE-1:01-049, 4 May 2001.

[4] Garnett, R., *ADTF Cryomodule Layout Clarification*, Los Alamos National Laboratory Memorandum, LANSCE-1:01-063, 16 July 2001.

[5] *Summary on LEDA RFQ Performance*, Accelerator Production of Tritium Project Technical Note, LA-UR-01-2670, July 2001.

[6] Rees, D., private communication.

[7] Krawczyk, F.L., *et al*., *Design of a Low-β, 2-Gap Spoke Resonator for the AAA Project*, Los Alamos National Laboratory Report, LA-UR-01-3218, 2001.

[8] Tajima, T., *et al*., "Results of Two LANL $\beta = 0.175$, 350-MHz, 2-Gap Spoke Cavities", *Proceedings of the 2003 Particle Accelerator Conference*, Portland, Oregon, 12-16 May 2003.

[9] Krawczyk, F.L., *RF Design of Spoke Resonators for the AAA Project*, Los Alamos National Laboratory Report, LA-UR-02-6872, Workshop on the Advanced Design of Spoke Resonators, Los Alamos, NM, USA (2002).

[10] Krawcyzk, F.L., *et al*., "An Integrated Design for a Beta = 0.175 Spoke Resonator and Associated Power Coupler", *Proceedings of the 8th European Particle Accelerator Conference*, Paris, France, 3-7 June 2002.

[11] Wangler, T., private communication.

[12] Krawcyzk, F.L., *et al*., "Design of a $\beta = 0.175$ 2-Gap Spoke Resonator", *Proceedings of the 10th Workshop on RF Superconductivity*, Tsukuba, Japan, September 2001.

[13] Shepard, K.W., P.N. Ostroumov and J.R. Delayen, "High-energy Ion Linacs Based on Superconducting Spoke Cavities", *Phys. Rev. ST – Accel. and Beams*, Vol. 6, 080101 (2003).

[14] Fuerst, J.D., *et al*., "Superconducting 345 MHz Two-Spoke Cavity for RIA", *Proceedings of the 2003 Particle Accelerator Conference*, Portland, Oregon, 12-16 May 2003.

[15] Zaplatain, E., *et al*., "Low-beta SC Cavity for ESS", *Proceedings of the 8th European Particle Accelerator Conference*, Paris, France, 3-7 June 2002.

TABLE OF CONTENTS